

UNCLASSIFIED

Defense Technical Information Center
Compilation Part Notice

ADP012510

TITLE: Formation and Structural Transitions of 3D Coulomb Crystals in
Dusty Plasmas

DISTRIBUTION: Approved for public release, distribution unlimited

This paper is part of the following report:

TITLE: Non-Neutral Plasma Physics 4. Workshop on Non-Neutral Plasmas
[2001] Held in San Diego, California on 30 July-2 August 2001

To order the complete compilation report, use: ADA404831

The component part is provided here to allow users access to individually authored sections of proceedings, annals, symposia, etc. However, the component should be considered within the context of the overall compilation report and not as a stand-alone technical report.

The following component part numbers comprise the compilation report:

ADP012489 thru ADP012577

UNCLASSIFIED

Formation and Structural Transitions of 3D Coulomb Crystals in Dusty Plasmas

Yasuaki Hayashi

*Department of Electronics and Information Science, Kyoto Institute of Technology
Matsugasaki, Sakyo-ku, Kyoto, Japan*

Abstract. 3D Coulomb crystals were formed in dusty plasmas using smaller fine particles growing in a methane/argon plasma. The structures were confirmed to be bct, fcc and hcp. The process of the structural transition from bct to fcc was analyzed and it was found that the transition occurred by the slip of crystal planes of bct(110), which are parallel to the fcc(111) planes. The direction of the slip was bct[110] and fcc[211]. This process of transition between the two crystal structures and the relations in crystal planes and axes agree with the martensitic transformation.

INTRODUCTION

The crystal ordering of charged fine particles in plasmas by the Coulomb or shielded Coulomb force is an attractive physical phenomenon. It was theoretically predicted in 1986 [1] and experimentally discovered in 1994 by three groups independently [2-4]. The lattice sizes are usually more than 100 μm and the arrangement of fine particles in a plasma can be observed even by the naked eye.

In dusty plasmas, i. e., plasma containing dust fine particles, larger monodisperse fine particles form the two-dimensional Coulomb crystal, a simple-hexagonal one. The formation is probably due to the effect of positively charged ion flow on fine particles sinking in a sheath region [5-7]. However, we found that three-dimensional Coulomb crystals can be formed by smaller fine particles, less than about 2 μm in diameter [8-10]. By the accurate size control of growing fine particles in plasmas, finely ordered three-dimensional (3D) Coulomb crystals were formed [11,12]. The three-dimensional structures, which were observed by the use of laser-light scattering and two CCD video cameras at the same time, were mainly body-centered tetragonal (bct) and face-centered cubic (fcc). The bct (110) and fcc(111) planes were parallel to an electrode. bct forms a part of face-centered orthorhombic (fco).

In this paper, the growth mechanism of monodisperse spherical fine particles, the formation of 3D Coulomb crystals, and the analyses of structural transition between two 3D crystals are described.

GROWTH OF MONODISPERSE FINE PARTICLES

Carbon fine particles were grown in a plasma of methane diluted in argon by coating the seeds of ultra-fine particles of graphite. The coated carbon material was found to be the hydrogenated amorphous carbon by its refractive index with the use of the in-situ measurement method of Mie-scattering ellipsometry [13,14].

The distribution function of ultra-fine particles is generally log-normal as

$$N(d) = \frac{1}{\sqrt{2\pi} d \ln \sigma} \exp \left\{ -\frac{[\ln d - \ln d_m]^2}{2 [\ln \sigma]^2} \right\}, \quad (1)$$

where d , d_m and σ represent particle size, the geometric mean size and the geometric standard deviation, respectively. If fine particles grow by coagulation, the type of distribution function does not change, although the geometric mean size and the standard deviation change [15]. However, when they grow by coating, a size distribution approaches the monodisperse one with growth as indicated by the following equation:

$$N(d) = \frac{1}{\sqrt{2\pi} (d - d_c) \ln \sigma} \exp \left\{ -\frac{[\ln(d - d_c) - \ln d_m]^2}{2 [\ln \sigma]^2} \right\}, \quad (2)$$

where d_c means the thickness of coated material on the seeds of ultra-fine particles.

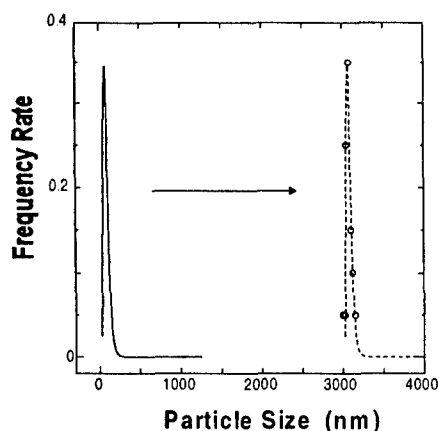


FIGURE 1. Size distribution of 20 grown fine particles (open circles). Solid line shows a log-normal distribution for $d_m=75\text{nm}$ and $\sigma=1.5$, and dotted line shows a distribution obtained by the shift of the log-normal distribution by 3000nm on the size axis.

Figure 1 shows a size distribution of 20 grown fine particles determined with the use of a scanning electron microscope (SEM). The dotted line in the figure shows a distribution indicated by eq.(2) for $d_m=75\text{nm}$, $\sigma=1.5$, and $d_c=3000\text{nm}$, which is obtained by the shift of a log-normal distribution of $d_m=75\text{nm}$ and $\sigma=1.5$. A SEM image of two grown carbon fine particles is shown in Fig.2 [16]. They indicate spherical shapes and uniform size. These results certify that monodisperse fine particles can be grown in the plasma.

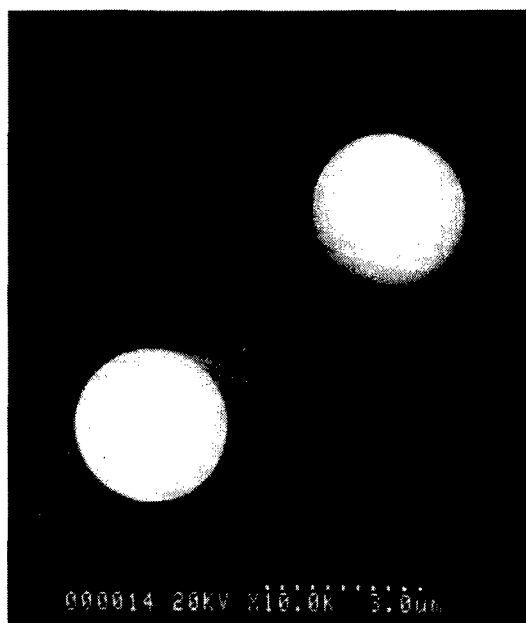


FIGURE 2. SEM image of grown carbon fine particles.

FORMATION OF 3D COULOMB CRYSTALS

In order to form three-dimensional Coulomb crystals and to analyze the structure, the size of growing fine particles was monitored and controlled using the Mie-scattering ellipsometry and two CCD video cameras, which were placed to acquire the top and side views of Coulomb crystal. An argon-ion-laser (wavelength:488 nm) and a diode-laser (690 nm) were used for the observation of particle arrangement by light scattering. Since the light intensity of the former laser is several-times higher than that of the latter, particle arrangements in a top view were indicated by the scattered light of argon-ion-laser. However, those in a side view were shown by that of a diode laser because an optical filter was put in front of the CCD.

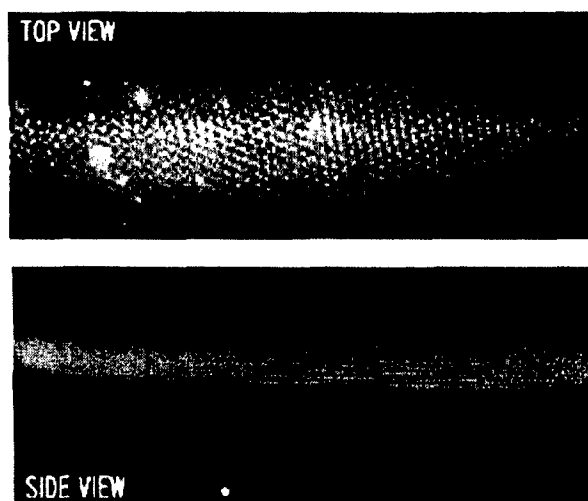


FIGURE 3. Top and side views of particle arrangement. Particle arrangements in the top view show those in the lowest few layers in the side view, and particle arrangements in the side view show those in the few vertical layers shown in the top view.

Figure 3 shows a top and a side views. Particle arrangements in the top view show those in the lowest few layers in the side view, and particle arrangements in the side view show those in the few vertical layers shown in the top view.

In fig.4, the time evolutions of the top and bottom positions of fine particle group are shown. As the bottom position almost did not change, the height of laser light needed not to be arranged during the observation.

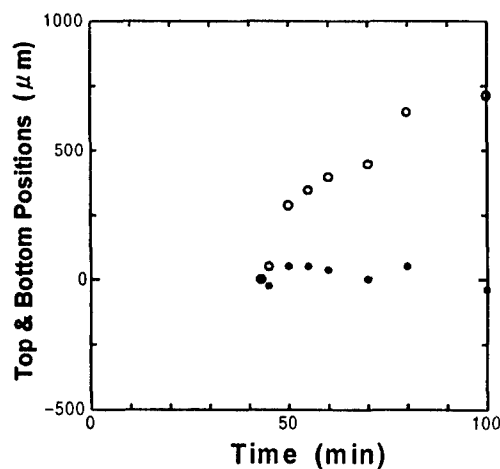


FIGURE 4. Time evolutions of top (open circles) and bottom (closed circles) positions of fine particle group.

Three-dimensional Coulomb crystals were formed by the control of the particle size around $2\text{ }\mu\text{m}$ in this experiment. A typical top-view image showing 3D Coulomb crystals is shown in Fig.5 [12]. In the image, regular triangle structures are observed in the middle and a square is found in the upper region. Since brighter spots indicate the fine particles in a lower layer, overlapping states of the lowest three layers can be known, i. e., fcc-like, hcp(hexagonal close-packed)-like and bcc(body-centered cubic)-like structures are seen in the right-middle, left-middle and upper regions, respectively. The distance between two horizontal layers were determined from the side-view image taken at the same time for the top-view. The ratio of the distance between the lowest two horizontal layers to the length of the triangle side was $0.82 : 1$ for the fcc-like structure. In comparison, the ratio for fcc is $\sqrt{2/3} : 1 = 0.816 : 1$. Furthermore, the ratio of the longer side length of the rectangle, to the shorter side length, to the distance between the lowest layer and the third lowest layer was $1.50 : 1 : 1.49$ for the bcc-like structure. Again in comparison, the ration for bcc is $\sqrt{2} : 1 : \sqrt{2} = 1.411 : 1 : 1.411$. Since the error of the values is less than 5 %, the former structure can be regarded as fcc with (111) planes parallel to an electrode and the latter regarded as bct (body-centered tetragonal) with (110) planes parallel to it. The hcp-like structure can be also regarded as hcp because the ratio of the distance between the lowest two horizontal layers to the length of a triangle side is equal to that of fcc.

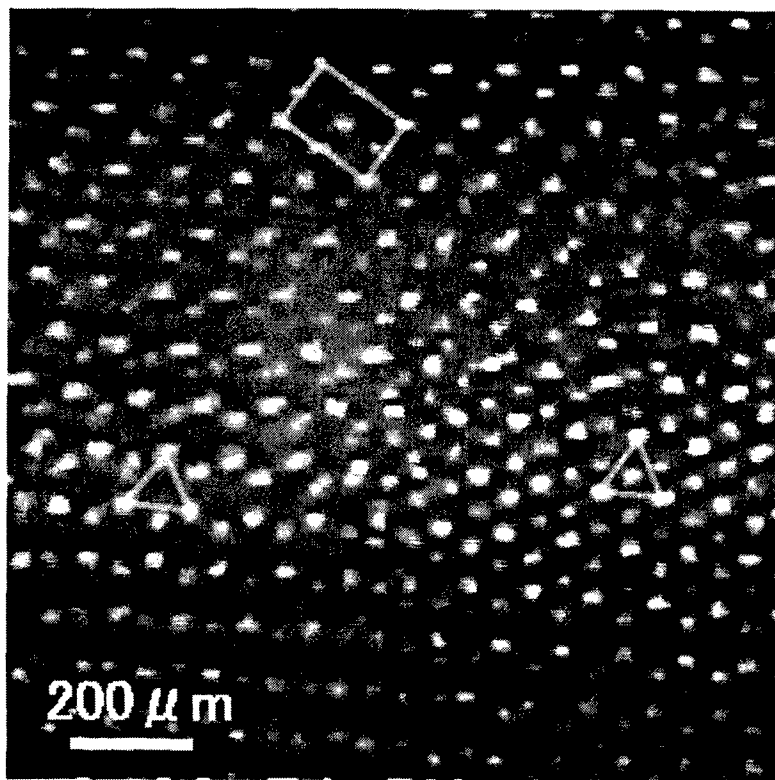


FIGURE 5. Top view of 3D Coulomb crystals.

STRUCTURAL TRANSITION BETWEEN TWO 3D COULOMB CRYSTALS

Structural transitions between bcc-like and fcc-like Coulomb crystals were distinguishably observed several times in the top view video images for 20 min. Figure 6 shows the top and the side views of the particle arrangements in the process of transition from bcc-like to fcc-like structure [12]. In the side views, it is recognized that the slip of the crystal planes occurred during the transition. Corresponding to the change of the side views, the gradual separation of the pairs of particles, which are in the lowest layer and the third lowest layer, is observed in the top views. Fine particles forming a bcc-like structure, which is equivalent to a fcc structure, pile up in alternate horizontal layers in the top view. Hence, the separation is observed alternately in the two directions of crystal axes.

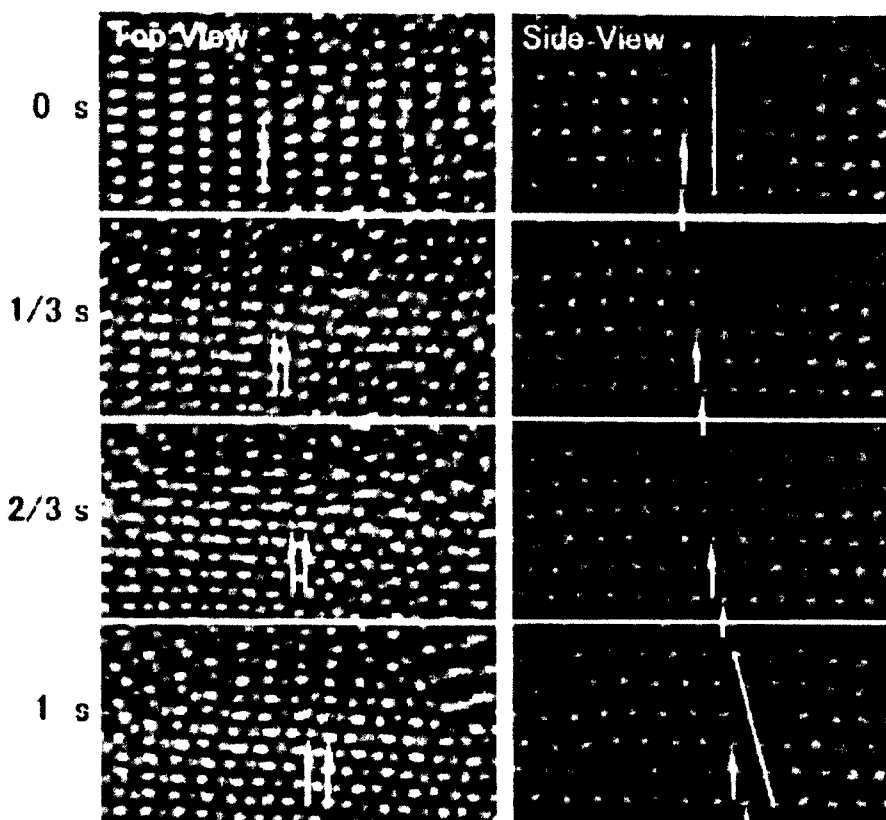


FIGURE 6. Top and side views of particle arrangements in process of transition from bcc-like to fcc-like structure in one second.

An explanatory drawing of the transition is shown in Fig.7. The direction of the slip is a $\text{fcc}[100]$ direction, which is equivalent to a $\text{bcc}[110]$ or $\text{bct}[110]$ direction for a special relation among the lattice satisfied.

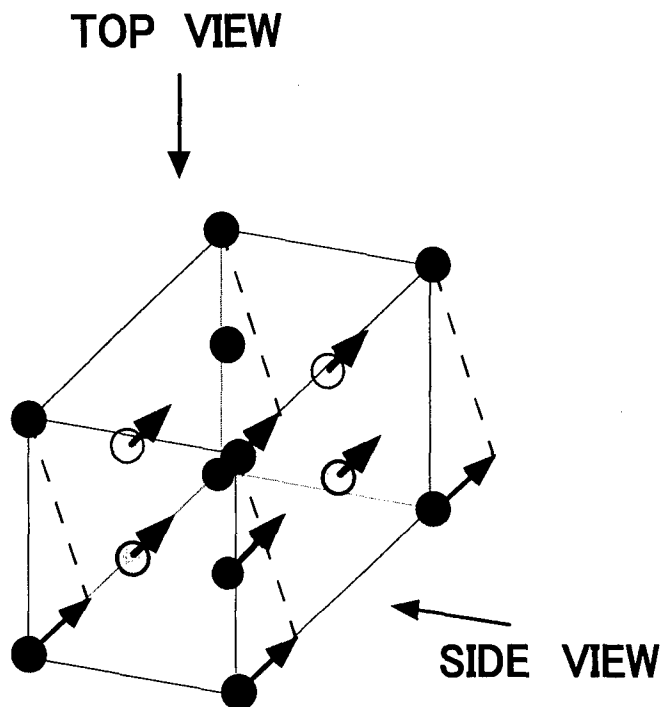


FIGURE 7. Explanatory drawing of transition between two 3D Coulomb crystals.

Figure 8 shows the change of particle arrangements of 49 particles in the lowest two layers in one second, corresponding to 0 sec and 1 sec images in the top views in Fig.6. It is seen in the figure at 1 s that each particle in the second lowest layer is at the center of three particles forming a regular triangle in the lowest layer as is seen in Fig.5. Similarly, the structural change of Coulomb crystals between bct and fcc can be explained by the slip of crystal planes, $\text{bct}(110)$ and $\text{fcc}(111)$. The direction of slip is $\text{bct}[110]$ and $\text{fcc}[211]$. This process of the transition between the two crystal structures and the relations of the crystal planes and the axes agree with the martensitic transformation of Nishiyama's scheme [17], which is observed when iron changes the structures between the austenite (fcc) and the martensite (bct or bcc) phases in the processes of hardening and tempering.

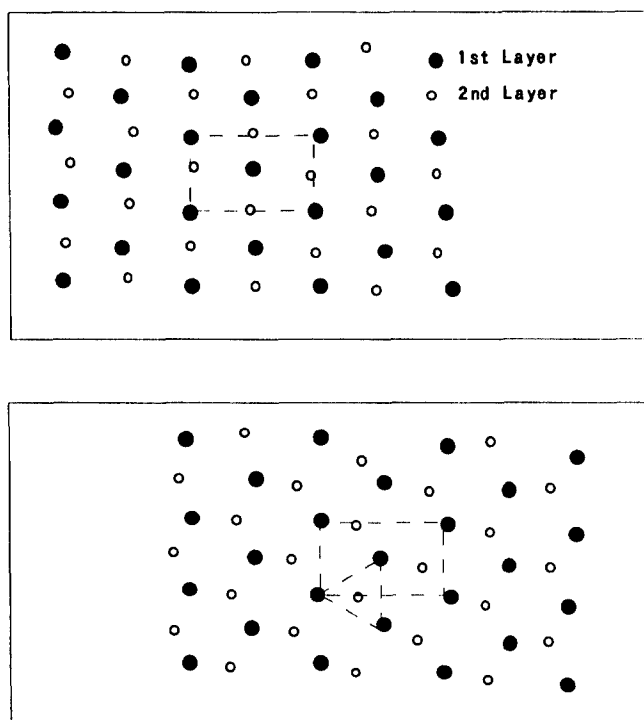


FIGURE 8. Change of particle arrangements of 49 particles in the lowest two layers in one second, corresponding to 0 s and 1 s images in the top views in Fig.6.

In order to understand the structural transition from Coulomb energy distribution, two non-dimensional parameters are defined. One is the ratio of one lattice constant to another in the plane of a slip, b/a , and the other is the ratio of slip distance to a lattice constant, $h/(b/2)$, as indicated in the upper figure of Fig.9. In the lower figure, Coulomb energy distribution per particle in units of $Q^2 / (4 \pi \epsilon_0 r_a)$, where Q and r_a are the charge of fine particles and the Wigner-Seitz radius, respectively, is shown as functions of b/a and $h/(b/2)$ for $r_a/r_D=3$, where r_D is the Debye-length. Since the energy is calculated using the inter-layer distance between horizontal planes being constant for the value of fcc, the point of minimum energy is seen at fcc but not at bcc in the figure.

The coordinates of each particle position indicated in Fig.8 were determined with the use of the Scion Image [18]. And the average values of the two non-dimensional parameters were calculated to be $b/a=1.664$ and $h/(b/2)=0.115$ at 0 sec and $b/a=1.709$ and $h/(b/2)=0.308$ at 1 sec. It is shown by the comparison of the result with Fig.9 that the change of particle arrangement is on the way to a fcc structure from a bct structure. The stability of the fcc structure was supported by the further analytical result of the transition: the value of $h/(b/2)$ did not exceed 0.34 [19].

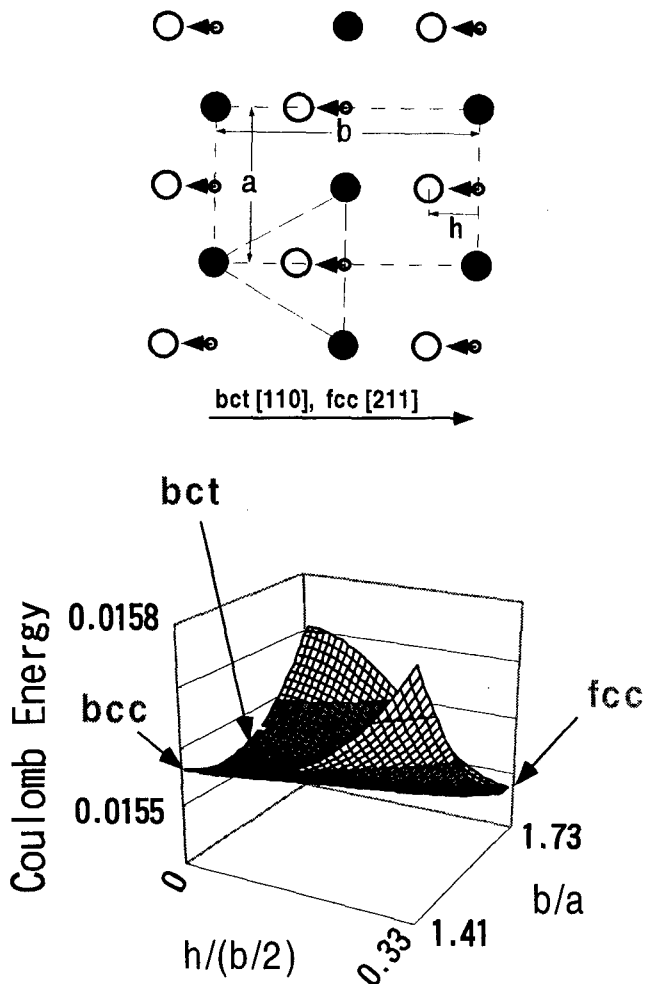


FIGURE 9. Coulomb energy distribution per particle in units of $Q^2 / (4 \pi \epsilon_0 r_a)$, where Q and r_a are the charge of fine particles and the Wigner-Seitz radius, respectively.

CONCLUSION

3D Coulomb crystals were formed in dusty plasmas using smaller fine particles growing in a methane/argon plasma. The structures were confirmed to be bct, fcc and hcp. The process of the structural transition from bct to fcc was analyzed and it was found that the transition occurred by the slip of crystal planes of bct(110), which are parallel to the fcc(111) planes. The direction of the slip was bct[110] and fcc[211]. This process of transition between the two crystal structures and the relations in crystal planes and axes agree with the martensitic transformation of Nishiyama's scheme. In conclusion, dusty plasma Coulomb crystals can be good models for real atomic crystals.

REFERENCES

1. Ikezi, H., *Phys. Fluids*, **29**, 1764-1766 (1986).
2. Hayashi, Y., and Tachibana, K., *Japan. J. Appl. Phys.* **33**, L804-L806 (1994).
3. Chu, J. H., and Lin, I., *Phys. Rev. Lett.* **72**, 4009-4012 (1994).
4. Thomas, H., Morfill, G. E., Demmel, V., Goree, J., Feuerbacher, B., and Mohlmann, D., *Phys. Rev. Lett.* **73**, 652-655 (1994).
5. Melandso, F., and Goree, J., *Phys. Rev. E*, **52**, 5312-5326 (1995).
6. Melzer, A., Schweigert, V. A., Schweigert, I. V., Homann, A., Peteres., S., and Piel, A., *Phys. Rev. E*, **54**, R46-R49 (1996).
7. Takahashi, K., Ohishi, T., Shimomai, K., Hayashi, Y., and Nishino, S., *Phys. Rev. E*, **58**, 7805-7811 (1998).
8. Hayashi, Y., and Tachibana, K., *J. Vac. Sci. Technol. A*, **14**, 506-510 (1996).
9. Hayashi, Y., Takahashi, K., and Tachibana, K., *Advanced in Dusty Plasmas*, Singapore: World Scientific, 1997, pp.153-162.
10. Hayashi, Y., and Takahashi, K., *Japan. J. Appl. Phys.* **36**, 4976-4979 (1997).
11. Hayashi, Y., *Phys. Rev. Lett.* **83**, 4764-4767 (1999).
12. Hayashi, Y., *Phys. Script.* **T89**, 112-116 (2001).
13. Hayashi, Y., and Tachibana, K., *Japan. J. Appl. Phys.* **33**, L476-L478 (1994).
14. Hayashi, Y., and Tachibana, K., *Japan. J. Appl. Phys.* **33**, 4208-4211 (1994).
15. Yoshida, T., Okuyama, K., Kousaka, Y., and Kida, Y., *J. Chem. Eng. Japan*, **8**, 317-322 (1975).
16. Hayashi, Y., and Tachibana, K., *Oyo Buturi* [in Japanese], **64**, 565-569 (1995).
17. Nishiyama, Z., *Sci. Rep. Tohoku. Univ.* **23**, 637- (1934).
18. <http://www.scioncorp.com>
19. Hayashi, Y., in preparation for publication.